

Bifurcation Dynamics and Control Mechanism of a Fractional–Order Delayed Brusselator Chemical Reaction Model

Changjin Xu^{a,b,*}, Dan Mu^c, Zixin Liu^c, Yicheng Pang^c
Chaouki Aouiti^d, Osman Tunç^e, Shabir Ahmad^f,
Anwar Zeb^g

^a*School of Mathematics and Statistics, Guizhou University of Finance
and Economics, Guiyang 550025, PR China*

^b*Guizhou Key Laboratory of Big Data Statistical Analysis, Guiyang
550025, PR China*

^c*School of Mathematics and Statistics, Guizhou University of Finance
and Economics, Guiyang 550004, PR China*

^d*University of Carthage, Faculty of Sciences of Bizerta, Department of
Mathematics, GAMA Laboratory LR21ES10 VBP W, Zarzouna 7021,
Bizerta, Tunisia*

^e*Department of Computer Programing, Baskale Vocational School, Van
Yuzuncu Yil University, Campus, 65080 Van-Turkey*

^f*Department of Mathematics, University of Malakand, Chakdara, Dir
Lower, Khyber Pakhtunkhwa, Pakistan*

^g*Department of Mathematics, COMSATS University Islamabad,
Abbottabad Campus, Abbottabad, 22060, Khyber, Pakhtunkhwa, Pakistan*

xcj403@126.com, md980929@126.com, xinxin905@126.com,

ypanggy@outlook.com, chaouki.aouiti@fsb.rnu.tn,

osmantunc89@gmail.com, habirahmad2232@gmail.com, anwar@cuiatd.edu.pk

(Received June 7, 2022)

*Corresponding author.

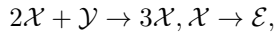
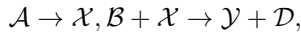
Abstract

Building differential dynamical systems to describe the changing relationship among chemical components is a vital aspect in chemistry. In this present manuscript, we put forward a new fractional-order delayed Brusselator chemical reaction model. By virtue of contraction mapping principle, we investigate the existence and uniqueness of the solution of fractional-order delayed Brusselator chemical reaction model. With the aid of mathematical analysis technique, we consider the non-negativeness of the solution of the fractional-order delayed Brusselator chemical reaction model. Making use of the theory of fractional-order dynamical system, we explore the stability and Hopf bifurcation issue of the fractional-order delayed Brusselator chemical reaction model. By designing a reasonable PD^c controller, we have availably controlled the time of emergence of Hopf bifurcation of the fractional-order delayed Brusselator chemical reaction model. A sufficient criterion guaranteeing the stability and the onset of Hopf bifurcation of the fractional-order controlled delayed Brusselator chemical reaction model is set up. Computer simulations are implemented to validate the theoretical findings. The derived fruits of this manuscript have great theoretical significance in controlling the concentrations of chemical substances.

1 Introduction

Differential equation has displayed a great application power in various areas such as physics, bioengineering, electronic technique, control technology, neural networks, chemistry, security cryptography and so on. Chemically, building a suitable differential equation to explore the changing law of different chemical components has become a central issue. During the past decades, a great deal of chemical models have been established and rich achievements have been achieved. For example, Zhabotinsky [1,2] considered the periodic dynamical behavior of the classical Belousov-Zhabotinsky reaction model(BZ reaction model). Kapral [3] discussed the complex dynamical phenomena of a discrete chemical reaction model. Xu et al. [4] explored the limit cycle of a fractional-order delayed Oregonator model. Xu et al. [5] revealed the effect of delay on the bifurcation of a fractional-order coupled Oregonator model. Din [6] studied the peculiarity of solution and bifurcation phenomenon of a chaotic chemical reaction system. For more related publications, one can see [7–10].

In 1968, Prigogine and Lefever [11] firstly explored the instability of a Brusselator chemical reaction model. Generally speaking, the Brusselator chemical reaction obeys the following steps:



where $\mathcal{A}, \mathcal{B}, \mathcal{X}, \mathcal{Y}, \mathcal{D}, \mathcal{E}$ represent different chemical reactants. If the concentrations of \mathcal{A} and \mathcal{B} keep unchange and reversible reactions will not happen, then the concentrations of \mathcal{X} and \mathcal{Y} obey the following rule:

$$\begin{cases} \frac{d[\mathcal{X}]}{dt} = \kappa_1[\mathcal{A}]_0 - \kappa_2[\mathcal{B}]_0[\mathcal{X}] + \kappa_3[\mathcal{X}]^2[\mathcal{Y}] - \kappa_4[\mathcal{X}], \\ \frac{d[\mathcal{Y}]}{dt} = \kappa_2[\mathcal{B}]_0[\mathcal{X}] - \kappa_3[\mathcal{X}]^2[\mathcal{Y}], \end{cases} \quad (1)$$

where $[\mathcal{A}], [\mathcal{B}], [\mathcal{X}], [\mathcal{Y}]$ stand for the concentrations of the chemical reactants $\mathcal{A}, \mathcal{B}, \mathcal{X}, \mathcal{Y}$, respectively. $\kappa_1, \kappa_2, \kappa_3, \kappa_4$ are real constants. By assuming that $[\mathcal{A}]$ and $[\mathcal{B}]$ are constants and equal to the initial values $[\mathcal{A}]_0$ and $[\mathcal{B}]_0$ of \mathcal{A} and \mathcal{B} , respectively. Making use of the following variable substitution:

$$[\mathcal{X}] \rightarrow v_1, [\mathcal{Y}] \rightarrow v_2, t \rightarrow t\kappa_3, a = \frac{[\mathcal{A}]_0\kappa_1}{\kappa_3}, b = \frac{[\mathcal{B}]_0\kappa_2}{\kappa_3}, \kappa_3 = \kappa_4,$$

then we get the following system:

$$\begin{cases} \frac{dv_1}{dt} = a - (1+b)v_1 + v_1^2v_2, \\ \frac{dv_2}{dt} = bv_1 - v_1^2v_2, \end{cases} \quad (2)$$

where $a > 0$ and $b > 0$ are proportional to the concentrations of \mathcal{A} and \mathcal{B} , respectively; The state variables v_1 and v_2 are proportional to \mathcal{X}, \mathcal{Y} , respectively. In details, we refer the readers to [12–14].

Time delay is a very important component in describing the dynamical behavior of lots of chemical reaction models. Generally speaking, the variation of the concentrations of the chemical reactants not only rely on the current time, but also rely on the past time. Thus time delay often

exists in chemical reaction models. Based on this viewpoint, we assume that the concentrations of \mathcal{A} and \mathcal{B} are affected by the chemical reactant \mathcal{Y} in the past period of time, then we can establish the following delayed Brusselator chemical reaction model:

$$\begin{cases} \frac{dv_1}{dt} = a - (1 + b)v_1 + v_1^2 v_2(t - \vartheta), \\ \frac{dv_2}{dt} = bv_1 - v_1^2 v_2(t - \vartheta), \end{cases} \quad (3)$$

where $\vartheta > 0$ is a time delay.

In addition, we would like to point out that fractional-order dynamical model is a more effective tool to describe the authentic natural law in objective world than the integer-order dynamical model due to the great advantage of fractional-order dynamical equation in the memory and hereditary function of various materials and development process [15, 16]. Nowadays, the exploration on fractional-order dynamical model has attracted great interest from lots of scholars in natural science and social science due to its potential application value in many subjects such as viscoelasticity, biological medical treatment, economics, control engineering, chemical engineering, neural networks and so on [17–20]. Recently, rich research results on fractional-order dynamical models have been published. For example, Xu et al. [21] revealed the impact of two different delays on the Hopf bifurcation of a fractional order bank data model. Xiao et al. [22] explored the Hopf bifurcation of a fractional-order small-world networks with time delays via fractional-order PD controller. Yousef et al. [23] dealt with the existence, uniqueness, non-negativity, boundedness of the solutions, global stability, Hopf bifurcation and persistence of a fractional-order prey-predator model. Shafiya and Nagamani [24] set up a finite-time passivity criteria of fractional-order delayed neural networks via Lyapunov function approach. In details, one can see [25–28]. Especially, delay-driven Hopf bifurcation plays a vital role in fractional-order dynamical systems. How to reveal the impact of delay on the Hopf bifurcation of fractional-order dynamical systems has become a hot issue. In addition, how to design a suitable controller to control the stability region and the onset of Hop bifurcation for fractional-order dynamical systems is

an interesting issue. In recent years, there are some publications on this aspect(see [29–31]). However, only very few papers on Hopf bifurcation of fractional-order chemical reaction models. What is the impact of delay on the stability and bifurcation of fractional-order chemical reaction models? How to control the stability and Hopf bifurcation? This is a problem that we must try to solve. In order to explore the effect of delay on the concentrations of the different chemical reactants, design suitable controllers to control the concentrations of the different chemical reactants, based on the analysis above, we propose the following fractional-order delayed Brusselator chemical reaction model and explore its Hopf bifurcation and Hopf bifurcation control aspect:

$$\begin{cases} \frac{d^\varsigma v_1}{dt^\varsigma} = a - (1 + b)v_1 + v_1^2 v_2(t - \vartheta), \\ \frac{d^\varsigma v_2}{dt^\varsigma} = bv_1 - v_1^2 v_2(t - \vartheta), \end{cases} \quad (4)$$

where $0 < \varsigma \leq 1$.

The primary objective of this manuscript are expressed as follows: **(a)** Probe into the stability and emergence of Hopf bifurcation of the fractional-order delayed Brusselator chemical reaction model (4); **(b)** Design a suitable PD^ς controller to control the stability region and the time of emergence of Hopf bifurcation of the fractional-order delayed Brusselator chemical reaction model (4).

The key contributions of this manuscript are expressed as follows:

- (1)** Based on the previous publications, a novel fractional-order delayed Brusselator chemical reaction model is proposed to better describe the memory and hereditary trait of the concentrations of the chemical reactants.
- (2)** A delay-independent stability and bifurcation condition of the fractional-order delayed Brusselator chemical reaction model (4) is built. The influence of delay on the stability and bifurcation of the fractional-order delayed Brusselator chemical reaction model (4) is clearly displayed.
- (3)** An accurate PD^ς controller is designed to control the stability region and the time of emergence of Hopf bifurcation of the fractional-order de-

layed Brusselator chemical reaction model (4).

④ So far, the exploration on Hopf bifurcation and Hopf bifurcation of fractional-order delayed Brusselator chemical reaction model is very scarce.

This manuscript is arranged as follows. Part 2 give some basic principle about fractional-order dynamical system. Part 3 explores the existence and uniqueness and non-negativeness of the solution to model (4). Part 4 sets up a stability and Hopf bifurcation condition of model (4). Part 5 probes into the bifurcation control issue via PD^ς controller. Part 6 presents the computer simulation plots to support the established key conclusions. Part 7 finishes this manuscript.

2 Preliminaries

In this part, several essential definitions and lemmas on fractional-order differential equation are prepared.

Definition 2.1. [32] *Define the fractional integral of order ς of the function $h(\nu)$ as follows*

$$\mathcal{I}^\varsigma h(\nu) = \frac{1}{\Gamma(\varsigma)} \int_{\nu_0}^{\nu} (\nu - s)^{\varsigma-1} h(s) ds,$$

where $\nu \geq \nu_0, \varsigma > 0$, and $\Gamma(s) = \int_0^\infty \nu^{s-1} e^{-\nu} d\nu$ denotes the Gamma function.

Definition 2.2. [32] *Assume that $h(\nu) \in C([\nu_0, \infty), R)$. The Caputo fractional-order derivative of order ς of $h(\nu)$ is given by*

$$\mathcal{D}^\varsigma h(\nu) = \frac{1}{\Gamma(l - \varsigma)} \int_{\nu_0}^{\nu} \frac{h^{(m)}(s)}{(\xi - s)^{\varsigma-m+1}} ds,$$

where $\nu \geq \nu_0$ and m denotes a positive integer satisfying $m - 1 \leq \varsigma < m$. Especially, if $0 < \varsigma < 1$, then

$$\mathcal{D}^\varsigma h(\nu) = \frac{1}{\Gamma(1 - \varsigma)} \int_{\nu_0}^{\nu} \frac{h'(s)}{(\nu - s)^\varsigma} ds.$$

Definition 2.3. [33] Consider the following fractional-order system:

$$\mathcal{D}^\varsigma v_i(t) = g_i(v_i(t)), i = 1, 2, \dots, k, \quad (5)$$

where $\varrho \in (0, 1]$, $v_i(t) = (v_1(t), v_2(t), \dots, v_h(t))$, $g_i(t) = (g_1(t), g_2(t), \dots, g_k(t))$. Then $(v_1^*, v_2^*, \dots, v_k^*)$ is said to be the equilibrium point of system (5) if $g_i(v_i^*) = 0$.

Lemma 2.1. [34] Let $\varsigma \in (0, 1]$ and $g(t) \in C[\alpha_1, \alpha_2]$ and $\mathcal{D}^\varsigma g(t) \in C[\alpha_1, \alpha_2]$. If $\mathcal{D}^\varsigma g(t) \geq 0, t \in (\alpha_1, \alpha_2)$, then $g(t)$ is a non-decreasing function for $t \in (\alpha_1, \alpha_2)$. If $\mathcal{D}^\varsigma g(t) \leq 0, t \in (\alpha_1, \alpha_2)$, then $g(t)$ is a non-increasing function for $t \in (\alpha_1, \alpha_2)$.

Lemma 2.2. [35] Consider the fractional-order system $\mathcal{D}^\varsigma w = \mathcal{P}w, w(0) = w_0$ where $0 < \varsigma < 1, w \in R^h, \mathcal{P} \in R^{h \times h}$. Let $\chi_l (l = 1, 2, \dots, h)$ be the root of the characteristic equation of $\mathcal{D}^\varsigma w = \mathcal{P}w$. Then system $\mathcal{D}^\varsigma w = \mathcal{P}w$ is asymptotically stable $\Leftrightarrow |\arg(\chi_l)| > \frac{\varsigma\pi}{2} (l = 1, 2, \dots, h)$. Furthermore, this system is stable $\Leftrightarrow |\arg(\chi_l)| > \frac{\varsigma\pi}{2} (l = 1, 2, \dots, h)$ and every critical eigenvalue obeying $|\arg(\chi_l)| = \frac{\varsigma\pi}{2} (l = 1, 2, \dots, h)$ possesses geometric multiplicity one.

Lemma 2.3. [36] For the fractional-order system $\mathcal{D}^\varsigma u(t) = \mathcal{P}_1 w(t) + \mathcal{P}_2 w(t - \vartheta)$, where $w(t) = \omega(t), t \in [-\vartheta, 0], \varsigma \in (0, 1], w \in R^n, \mathcal{P}_1, \mathcal{P}_2 \in R^{n \times n}$. Then the characteristic equation of the system is $\det |s^\varsigma \mathcal{I} - \mathcal{P}_1 - \mathcal{P}_2 e^{-s\vartheta}| = 0$. Then the zero solution of the model is asymptotically stable if every root of the equation $\det |s^\varsigma \mathcal{I} - \mathcal{P}_1 - \mathcal{P}_2 e^{-s\vartheta}| = 0$ possesses negative real roots.

3 Existence and uniqueness, non-negativeness of solution

In this section, we will study the existence and uniqueness, non-negativeness of the solution of model (4).

Theorem 3.1. Set $\Pi = \{v_1, v_2\} \in R^2 : \max\{|v_1|, |v_2|\} \leq \mathcal{V}\}$, where $\mathcal{V} > 0$ is a constant. $\forall (v_{10}, v_{20}) \in \Pi$, the model (4) with the initial value (v_{10}, v_{20}) has a unique solution $V = (v_1, v_2) \in \Pi$.

Proof. Define the following mapping:

$$f(V) = (f_1(V), f_2(V)), \quad (6)$$

where

$$\begin{cases} f_1(V) = a - (1+b)v_1 + v_1^2 v_2(t - \vartheta), \\ f_2(V) = bv_1 - v_1^2 v_2(t - \vartheta). \end{cases} \quad (7)$$

$\forall V, \tilde{V} \in \Pi$, we get

$$\begin{aligned} & \|f(V) - f(\tilde{V})\| \\ &= |a - (1+b)v_1 + v_1^2 v_2(t - \vartheta) - [a - (1+b)\tilde{v}_1 + \tilde{v}_1^2 \tilde{v}_2(t - \vartheta)]| \\ &\quad + |bv_1 - v_1^2 v_2(t - \vartheta) - [b\tilde{v}_1 - \tilde{v}_1^2 \tilde{v}_2(t - \vartheta)]| \\ &\leq |(1+b)(v_1(t) - \tilde{v}_1(t)) + [v_1^2 v_2(t - \vartheta) - \tilde{v}_1^2 \tilde{v}_2(t - \vartheta)]| \\ &\quad + |b(v_1(t) - \tilde{v}_1(t)) - [v_1^2 v_2(t - \vartheta) - \tilde{v}_1^2 \tilde{v}_2(t - \vartheta)]| \\ &\leq (1+b)|v_1(t) - \tilde{v}_1(t)| + \mathcal{V}^2 |v_2(t) - \tilde{v}_2(t)| + \mathcal{V}^2 |v_2(t) - \tilde{v}_2(t)| \\ &\quad + 2\mathcal{V}^3 |v_1(t) - \tilde{v}_1(t)| + b|v_1(t) - \tilde{v}_1(t)| + \mathcal{V}^2 |v_2(t) - \tilde{v}_2(t)| \\ &\quad + \mathcal{V}^2 |v_2(t) - \tilde{v}_2(t)| + 4\mathcal{V}^3 |v_1(t) - \tilde{v}_1(t)| \\ &= (1 + 2b + 4\mathcal{V}^3) |v_1(t) - \tilde{v}_1(t)| + 4\mathcal{V}^2 |v_2(t) - \tilde{v}_2(t)| \\ &\leq \mathcal{A} \|V - \tilde{V}\|, \end{aligned} \quad (8)$$

where

$$\mathcal{A} = \max\{1 + 2b + 4\mathcal{V}^3, 4\mathcal{V}^2\}. \quad (9)$$

Then $f(V)$ obeys Lipschitz condition with respect to V (refer to [37]). Thus Theorem 3.1 holds. \blacksquare

Theorem 3.2. *Every solution of model (4) beginning with R_+^2 is non-negative.*

Proof. Assume that $V(t_0) = (v_1(t_0), v_2(t_0))$ is the initial value of model (1.4). Suppose that there exists a constant t_* satisfying $t_0 < t < t_*$ such

that

$$\begin{cases} v_1(t) = 0, t_0 < t < t_*, \\ v_1(t_*) = 0, \\ v_1(t_*^+) < 0. \end{cases} \quad (10)$$

According to model (4), we have

$$\mathcal{D}^\varsigma v_1(t)|_{v_1(t_*)=0} = a > 0. \quad (11)$$

Applying Lemma 2.1, we know that $v_1(t_*^+) > 0$, which is a contradiction (see [38]). Thus $v_1(t) \geq 0$ for $t \geq t_0$. In a similar way, we can easily prove that $v_2(t) \geq 0$ for $t \geq t_0$. ■

4 Bifurcation exploration of model (4)

In this section, we will investigate the stability and Hopf bifurcation of model (4). Obviously, model (4) has unique positive equilibrium points $E(a, \frac{b}{a})$. Let

$$\begin{cases} \bar{v}_1(t) = v_1(t) - a, \\ \bar{v}_2(t) = v_2(t) - \frac{b}{a}, \end{cases} \quad (12)$$

then

$$\begin{cases} v_1(t) = \bar{v}_1(t) + a, \\ v_2(t) = \bar{v}_2(t) + \frac{b}{a}. \end{cases} \quad (13)$$

Substituting (13) into (4), we have

$$\begin{cases} \frac{d^\varsigma \bar{v}_1}{dt^\varsigma} = a - (1+b)(\bar{v}_1(t) + a) + (\bar{v}_1(t) + a)^2 \left(\bar{v}_2(t - \vartheta) + \frac{b}{a} \right), \\ \frac{d^\varsigma \bar{v}_2}{dt^\varsigma} = b(\bar{v}_1(t) + a) - (\bar{v}_1(t) + a)^2 \left(\bar{v}_2(t - \vartheta) + \frac{b}{a} \right). \end{cases} \quad (14)$$

The linear system of Eq. (14) around $(0, 0)$ can be expressed as

$$\begin{cases} \frac{d^\varsigma \bar{v}_1}{dt^\varsigma} = (b-1)\bar{v}_1(t) + a^2\bar{v}_2(t - \vartheta), \\ \frac{d^\varsigma \bar{v}_2}{dt^\varsigma} = -b\bar{v}_1(t) - a^2\bar{v}_2(t - \vartheta). \end{cases} \quad (15)$$

The characteristic equation of system (15) is

$$\det \begin{bmatrix} s^\varsigma - (b-1) & -a^2 e^{-s\vartheta} \\ b & s^\varsigma + a_2 e^{-s\vartheta} \end{bmatrix} = 0, \quad (16)$$

which leads to

$$s^{2\varsigma} - (b-1)s^\varsigma + a^2(s^\varsigma + 1)e^{-s\vartheta} = 0, \quad (17)$$

Now we give the following hypothesis:

$$(H_1) \quad a^2 - b + 1 > 0.$$

Lemma 4.1. *If (H_1) holds, then the positive equilibrium point $E(a, \frac{b}{a})$ of model (4) is locally asymptotically stable.*

Proof. When $\vartheta = 0$, then (17) becomes

$$\lambda^2 + (a^2 - b + 1)\lambda + a^2 = 0. \quad (18)$$

According to (H_1) , one derives that the two roots λ_l of (18) satisfy $|\arg(\lambda_1)| > \frac{\varsigma\pi}{2}$, $|\arg(\lambda_2)| > \frac{\varsigma\pi}{2}$. By Lemma 2.2, one can conclude that the positive equilibrium point $E(a, \frac{b}{a})$ of model (4) is locally asymptotically stable.

The proof ends. ■

Suppose that $s = i\mu = \mu \left(\cos \frac{\pi}{2} + i \sin \frac{\pi}{2} \right)$ is a root of (17). Then

$$\begin{aligned} & \mu^{2\varsigma} (\cos \varsigma\pi + i \sin \varsigma\pi) - (b-1)\mu^\varsigma \left(\cos \frac{\varsigma\pi}{2} + i \sin \frac{\varsigma\pi}{2} \right) \\ & + a^2 \left[\mu^\varsigma \left(\cos \frac{\varsigma\pi}{2} + i \sin \frac{\varsigma\pi}{2} \right) + 1 \right] (\cos \mu\vartheta - i \sin \mu\vartheta) = 0, \end{aligned} \quad (19)$$

which leads to

$$\begin{cases} \alpha_1 \cos \mu\vartheta + \alpha_2 \sin \mu\vartheta = \alpha_3, \\ \alpha_2 \cos \mu\vartheta - \alpha_1 \sin \mu\vartheta = \alpha_4, \end{cases} \quad (20)$$

where

$$\begin{cases} \alpha_1 = a^2 \left(\mu^\zeta \cos \frac{\zeta\pi}{2} + 1 \right), \\ \alpha_2 = a^2 \mu^\zeta \sin \frac{\zeta\pi}{2}, \\ \alpha_3 = -\mu^{2\zeta} \cos \zeta\pi + (b-1)\mu^\zeta \cos \frac{\zeta\pi}{2}, \\ \alpha_4 = -\mu^{2\zeta} \sin \zeta\pi + (b-1)\mu^\zeta \sin \frac{\zeta\pi}{2}. \end{cases} \quad (21)$$

By (20), one gets

$$\alpha_1^2 + \alpha_2^2 = \alpha_3^2 + \alpha_4^2. \quad (22)$$

which leads to

$$\mu^{4\zeta} + c_1\mu^{3\zeta} + c_2\mu^{2\zeta} + c_3\mu^\zeta + c_4 = 0, \quad (23)$$

where

$$\begin{cases} c_1 = -2(b-1) \left(\cos \zeta\pi \cos \frac{\zeta\pi}{2} + \sin \zeta\pi \sin \frac{\zeta\pi}{2} \right), \\ c_2 = (b-1)^2 - a^4, \\ c_3 = -a^4 \cos \frac{\zeta\pi}{2}, \\ c_4 = -a^4. \end{cases} \quad (24)$$

Let

$$\Psi(\mu) = \mu^{4\zeta} + c_1\mu^{3\zeta} + c_2\mu^{2\zeta} + c_3\mu^\zeta + c_4. \quad (25)$$

Notice that $c_4 < 0$, $\frac{d\Psi(\mu)}{d\mu} > 0$, for all $\mu > 0$, then Eq.(23) owns at least one positive real root. Thus Eq.(17) owns at least one pair of purely roots.

Assume that Eq.(23) has four real roots labeled by $\mu_i > 0 (j = 1, 2, 3, 4)$.

By (20), we derive

$$\vartheta_i^h = \frac{1}{\mu_i} \left[\arccos \left(\frac{\alpha_1\alpha_3 + \alpha_2\alpha_4}{\alpha_1^2 - \alpha_2^2} \right) + 2h\pi \right], \quad (26)$$

where $h = 0, 1, 2, \dots, i = 1, 2, 3, 4$. Let

$$\vartheta_0 = \min_{i=1,2,3,4} \{\vartheta_i^0\}, \mu_0 = \mu|_{\vartheta=\vartheta_0}. \quad (27)$$

Now we give the following hypothesis:

(H₂) $\mathcal{U}_1\mathcal{V}_1 + \mathcal{U}_2\mathcal{V}_2 > 0$, where

$$\left\{ \begin{array}{l} \mathcal{U}_1 = 2\varsigma\mu_0^{2\varsigma-1} \cos \frac{(2\varsigma-1)\pi}{2} - (b-1)\varsigma\mu_0^{\varsigma-1} \cos \frac{(\varsigma-1)\pi}{2} \\ \quad + a^2\varsigma\mu_0^{\varsigma-1} \cos \frac{(\varsigma-1)\pi}{2} \cos \mu_0\vartheta_0 \\ \quad + a^2\varsigma\mu_0^{\varsigma-1} \sin \frac{(\varsigma-1)\pi}{2} \sin \mu_0\vartheta_0, \\ \mathcal{U}_2 = 2\varsigma\mu_0^{2\varsigma-1} \sin \frac{(2\varsigma-1)\pi}{2} - (b-1)\varsigma\mu_0^{\varsigma-1} \sin \frac{(\varsigma-1)\pi}{2} \\ \quad - a^2\varsigma\mu_0^{\varsigma-1} \cos \frac{(\varsigma-1)\pi}{2} \sin \mu_0\vartheta_0 \\ \quad + a^2\varsigma\mu_0^{\varsigma-1} \sin \frac{(\varsigma-1)\pi}{2} \cos \mu_0\vartheta_0, \\ \mathcal{V}_1 = a^2 \left(\mu_0^\varsigma \cos \frac{\varsigma\pi}{2} + 1 \right) \mu_0 \sin \mu_0\vartheta_0 - a^2\mu_0^{\varsigma+1} \sin \frac{\varsigma\pi}{2} \cos \mu_0\vartheta_0, \\ \mathcal{V}_2 = a^2 \left(\mu_0^\varsigma \cos \frac{\varsigma\pi}{2} + 1 \right) \mu_0 \cos \mu_0\vartheta_0 + a^2\mu_0^{\varsigma+1} \sin \frac{\varsigma\pi}{2} \sin \mu_0\vartheta_0. \end{array} \right. \quad (28)$$

Lemma 4.2. *Suppose that $s(\vartheta) = \tau_1(\vartheta) + i\tau_2(\vartheta)$ is the root of (17) around $\vartheta = \vartheta_0$ such that $\tau_1(\vartheta_0) = 0, \tau_2(\vartheta_0) = \mu_0$, then $\operatorname{Re} \left[\frac{ds}{d\vartheta} \right]_{\vartheta=\vartheta_0, \mu=\mu_0} > 0$.*

Proof. Applying (17), we derive

$$\begin{aligned} & [2\varsigma s^{2\varsigma-1} - (b-1)\varsigma s^{\varsigma-1}] \frac{ds}{d\vartheta} + a^2\varsigma s^{\varsigma-1} e^{-s\vartheta} \frac{ds}{d\vartheta} \\ & - e^{-s\vartheta} \left(\frac{ds}{d\vartheta} \vartheta + s \right) a^2 (s^\varsigma + 1) = 0. \end{aligned} \quad (29)$$

By (29), one gets

$$\left(\frac{ds}{d\vartheta} \right)^{-1} = \frac{\mathcal{U}}{\mathcal{V}} - \frac{\vartheta}{s}, \quad (30)$$

where

$$\left\{ \begin{array}{l} \mathcal{U} = 2\varsigma s^{2\varsigma-1} - (b-1)\varsigma s^{\varsigma-1} + a^2\varsigma s^{\varsigma-1} e^{-s\vartheta}, \\ \mathcal{V} = e^{-s\vartheta} s a^2 (s^\varsigma + 1). \end{array} \right. \quad (31)$$

Then

$$\operatorname{Re} \left[\left(\frac{ds}{d\vartheta} \right)^{-1} \right] = \operatorname{Re} \left[\left(\frac{\mathcal{U}}{\mathcal{V}} \right)^{-1} \right]. \quad (32)$$

Thus

$$\operatorname{Re} \left[\left(\frac{ds}{d\vartheta} \right)^{-1} \right]_{\vartheta=\vartheta_0, \mu=\mu_0} = \frac{\mathcal{U}_1\mathcal{V}_1 + \mathcal{U}_2\mathcal{V}_2}{\mathcal{V}_1^2 + \mathcal{V}_2^2}. \quad (33)$$

By (H_2) , ones has

$$\operatorname{Re} \left[\left(\frac{ds}{d\vartheta} \right)^{-1} \right]_{\vartheta=\vartheta_0, \mu=\mu_0} > 0. \quad (34)$$

The proof of Lemma 4.2 ends. ■

By virtue of the exploration above, the following result can be easily derived.

Theorem 4.1. *Under the hypotheses (H_1) and (H_2) , the positive equilibrium point $E(a, \frac{b}{a})$ of model (4) is locally asymptotically stable if ϑ lies in the range $[0, \vartheta_0)$ and a Hopf bifurcation will happen around $E(a, \frac{b}{a})$ if ϑ exceeds the critical value ϑ_0 .*

5 Bifurcation control of model (4) via PD^s controller

In this section, we are to apply PD^s controller to control the Hopf bifurcation of model (4). The PD^s controller is designed as follows:

$$u(t) = \varrho_p \left(v_2(t - \vartheta) - \frac{b}{a} \right) + \varrho_d \frac{d^s \left(v_2(t) - \frac{b}{a} \right)}{dt^s}, \quad (35)$$

where ϱ_p and $\varrho_d \neq 1$ represent the proportional control parameter and the derivative control parameter, respectively, ϑ stands for a delay. Adding (35) to the second equation of model (4), one gets

$$\begin{cases} \frac{d^s v_1}{dt^s} = a - (1 + b)v_1 + v_1^2 v_2(t - \vartheta), \\ \frac{d^s v_2}{dt^s} = bv_1 - v_1^2 v_2(t - \vartheta) + \varrho_p \left(v_2(t - \vartheta) - \frac{b}{a} \right) + \varrho_d \frac{d^s \left(v_2(t) - \frac{b}{a} \right)}{dt^s}. \end{cases} \quad (36)$$

System (36) is equivalent to

$$\begin{cases} \frac{d^s v_1}{dt^s} = a - (1+b)v_1 + v_1^2 v_2(t-\vartheta), \\ \frac{d^s v_2}{dt^s} = \frac{1}{1-\varrho_d} \left[b v_1 - v_1^2 v_2(t-\vartheta) + \varrho_p \left(v_2(t-\vartheta) - \frac{b}{a} \right) \right]. \end{cases} \quad (37)$$

Clearly, system (37) has the same equilibrium point as that in model (4). Namely, system (37) has the unique positive equilibrium point $E(a, \frac{b}{a})$. The linear system of Eq. (37) around $E(a, \frac{b}{a})$ can be expressed as

$$\begin{cases} \frac{d^s \bar{v}_1}{dt^s} = d_1 \bar{v}_1(t) + d_2 \bar{v}_2(t-\vartheta), \\ \frac{d^s \bar{v}_2}{dt^s} = d_3 \bar{v}_1(t) + d_4 \bar{v}_2(t-\vartheta), \end{cases} \quad (38)$$

where

$$\begin{cases} d_1 = (b-1) \\ d_2 = a^2, \\ d_3 = -\frac{b}{1-\varrho_d}, \\ d_4 = -\frac{a^2 - \varrho_p}{1-\varrho_d}. \end{cases} \quad (39)$$

The characteristic equation of system (38) is

$$\det \begin{bmatrix} s^\zeta - d_1 & -d_2 e^{-s\vartheta} \\ -d_3 & s^\zeta - d_4 e^{-s\vartheta} \end{bmatrix} = 0, \quad (40)$$

which leads to

$$s^{2\zeta} + e_1 s^\zeta + (e_2 s^\zeta + e_3) e^{-s\vartheta} = 0, \quad (41)$$

where

$$\begin{cases} e_1 = -d_1 \\ e_2 = -d_4, \\ e_3 = d_1 d_4 - d_2 d_3. \end{cases} \quad (42)$$

Now we give the following hypothesis:

$$(H_3) \quad e_1 + e_2 > 0, e_3 > 0$$

Lemma 5.1. *If (H_3) holds, then the positive equilibrium point $E(a, \frac{b}{a})$ of model (37) is locally asymptotically stable.*

Proof. When $\vartheta = 0$, then (41) becomes

$$\lambda^2 + (e_1 + e_2)\lambda + e_3 = 0. \quad (43)$$

According to (H_3) , one derives that the two roots λ_i of (41) satisfy $|\arg(\lambda_1)| > \frac{\varsigma\pi}{2}$, $|\arg(\lambda_2)| > \frac{\varsigma\pi}{2}$. By Lemma 2.2, one can conclude that the positive equilibrium point $E(a, \frac{b}{a})$ of model (37) is locally asymptotically stable. The proof ends. \blacksquare

Suppose that $s = i\sigma = \sigma \left(\cos \frac{\pi}{2} + i \sin \frac{\pi}{2} \right)$ is a root of (41). Then

$$\begin{aligned} & \sigma^{2\varsigma} \left(\cos \varsigma\pi + i \sin \varsigma\pi \right) + e_1 \sigma^\varsigma \left(\cos \frac{\varsigma\pi}{2} + i \sin \frac{\varsigma\pi}{2} \right) \\ & + e_2 \left[\mu^\varsigma \left(\cos \frac{\varsigma\pi}{2} + i \sin \frac{\varsigma\pi}{2} \right) + e_3 \right] (\cos \sigma\vartheta - i \sin \sigma\vartheta) = 0, \end{aligned} \quad (44)$$

which leads to

$$\begin{cases} \beta_1 \cos \sigma\vartheta + \beta_2 \sin \sigma\vartheta = \beta_3, \\ \beta_2 \cos \sigma\vartheta - \beta_1 \sin \sigma\vartheta = \beta_4, \end{cases} \quad (45)$$

where

$$\begin{cases} \beta_1 = e_2 \left(\sigma^\varsigma \cos \frac{\varsigma\pi}{2} + e_3 \right), \\ \beta_2 = e_2 \sigma^\varsigma \sin \frac{\varsigma\pi}{2}, \\ \beta_3 = -\sigma^{2\varsigma} \cos \varsigma\pi - e_1 \sigma^\varsigma \cos \frac{\varsigma\pi}{2}, \\ \beta_4 = -\sigma^{2\varsigma} \sin \varsigma\pi - e_1 \sigma^\varsigma \sin \frac{\varsigma\pi}{2}. \end{cases} \quad (46)$$

By (5.11), one gets

$$\beta_1^2 + \beta_2^2 = \beta_3^2 + \beta_4^2. \quad (47)$$

which leads to

$$\sigma^{4\varsigma} + \varepsilon_1 \sigma^{3\varsigma} + \varepsilon_2 \sigma^{2\varsigma} + \varepsilon_3 \sigma^\varsigma + \varepsilon_4 = 0, \quad (48)$$

where

$$\begin{cases} \varepsilon_1 = 2e_1 \left(\cos \zeta \pi \cos \frac{\zeta \pi}{2} + \sin \zeta \pi \sin \frac{\zeta \pi}{2} \right), \\ \varepsilon_2 = e_1^2 - e_2^2, \\ \varepsilon_3 = 2e_2^2 e_3 \cos^2 \frac{\zeta \pi}{2}, \\ \varepsilon_4 = -e_2^2 e_3^2. \end{cases} \quad (49)$$

Let

$$\Phi(\sigma) = \sigma^{4\zeta} + \varepsilon_1 \sigma^{3\zeta} + \varepsilon_2 \sigma^{2\zeta} + \varepsilon_3 \sigma^\zeta + \varepsilon_4. \quad (50)$$

Notice that $\varepsilon_4 < 0$, $\frac{d\Phi(\sigma)}{d\sigma} > 0$, for all $\sigma > 0$, then Eq.(48) owns at least one positive real root. Thus Eq.(41) owns at least one pair of purely roots.

Assume that Eq.(48) has four real roots labeled by $\sigma_i > 0 (i = 1, 2, 3, 4)$.

By (45), we derive

$$\vartheta_i^h = \frac{1}{\sigma_i} \left[\arccos \left(\frac{\beta_1 \beta_3 + \beta_2 \beta_4}{\beta_1^2 + \beta_2^2} \right) + 2h\pi \right], \quad (51)$$

where $h = 0, 1, 2, \dots, i = 1, 2, 3, 4$. Let

$$\vartheta^0 = \min_{i=1,2,3,4} \{\vartheta_i^0\}, \sigma_0 = \mu|_{\vartheta=\vartheta^0}. \quad (52)$$

Now we give the following hypothesis:

(H_4) $\mathcal{S}_1 \mathcal{Z}_1 + \mathcal{S}_2 \mathcal{Z}_2 > 0$, where

$$\begin{cases} \mathcal{S}_1 = 2\zeta \sigma_0^{2\zeta-1} \cos \frac{(2\zeta-1)\pi}{2} + e_1 \zeta \sigma_0^{\zeta-1} \cos \frac{(\zeta-1)\pi}{2} \\ \quad + e_2 \zeta \sigma_0^{\zeta-1} \cos \frac{(\zeta-1)\pi}{2} \cos \sigma_0 \vartheta^0 \\ \quad + e_2 \zeta \sigma_0^{\zeta-1} \sin \frac{(\zeta-1)\pi}{2} \sin \sigma_0 \vartheta^0, \\ \mathcal{S}_2 = 2\zeta \sigma_0^{2\zeta-1} \sin \frac{(2\zeta-1)\pi}{2} + e_1 \zeta \sigma_0^{\zeta-1} \sin \frac{(\zeta-1)\pi}{2} \\ \quad - e_2 \zeta \sigma_0^{\zeta-1} \cos \frac{(\zeta-1)\pi}{2} \sin \sigma_0 \vartheta^0 \\ \quad + e_2 \zeta \sigma_0^{\zeta-1} \sin \frac{(\zeta-1)\pi}{2} \cos \sigma_0 \vartheta^0, \\ \mathcal{Z}_1 = \left(e_2 \sigma_0^\zeta \cos \frac{\zeta \pi}{2} + e_3 \right) \sigma_0 \sin \sigma_0 \vartheta^0 - e_2 \sigma_0^{\zeta+1} \cos \frac{\zeta \pi}{2} \cos \sigma_0 \vartheta^0, \\ \mathcal{Z}_2 = \left(e_2 \sigma_0^\zeta \cos \frac{\zeta \pi}{2} + e_3 \right) \sigma_0 \cos \sigma_0 \vartheta^0 + e_2 \sigma_0^{\zeta+1} \cos \frac{\zeta \pi}{2} \sin \sigma_0 \vartheta^0. \end{cases} \quad (53)$$

Lemma 5.2. *Suppose that $s(\vartheta) = \epsilon_1(\vartheta) + i\epsilon_2(\vartheta)$ is the root of (41) around $\vartheta = \vartheta^0$ such that $\epsilon_1(\vartheta_0) = 0, \epsilon_2(\vartheta_0) = \mu_0$, then $\text{Re} \left[\frac{ds}{d\vartheta} \right]_{\vartheta=\vartheta^0, \sigma=\sigma_0} > 0$.*

Proof. Applying (41), we derive

$$\begin{aligned} & [2\zeta s^{2\zeta-1} + e_1\zeta s^{\zeta-1}] \frac{ds}{d\vartheta} + e_2\zeta s^{\zeta-1} e^{-s\vartheta} \frac{ds}{d\vartheta} \\ & - e^{-s\vartheta} \left(\frac{ds}{d\vartheta} \vartheta + s \right) (e_2 s^\zeta + e_3) = 0. \end{aligned} \quad (54)$$

By (54), one gets

$$\left(\frac{ds}{d\vartheta} \right)^{-1} = \frac{\mathcal{S}}{\mathcal{Z}} - \frac{\vartheta}{s}, \quad (55)$$

where

$$\begin{cases} \mathcal{S} = 2\zeta s^{2\zeta-1} + e_1\zeta s^{\zeta-1} + e_2\zeta s^{\zeta-1} e^{-s\vartheta}, \\ \mathcal{Z} = e^{-s\vartheta} s (e_2 s^\zeta + e_3). \end{cases} \quad (56)$$

Then

$$\text{Re} \left[\left(\frac{ds}{d\vartheta} \right)^{-1} \right] = \text{Re} \left[\left(\frac{\mathcal{S}}{\mathcal{Z}} \right)^{-1} \right]. \quad (57)$$

Thus

$$\text{Re} \left[\left(\frac{ds}{d\vartheta} \right)^{-1} \right]_{\vartheta=\vartheta_0, \mu=\mu_0} = \frac{\mathcal{S}_1 \mathcal{Z}_1 + \mathcal{S}_2 \mathcal{Z}_2}{\mathcal{Z}_1^2 + \mathcal{Z}_2^2}. \quad (58)$$

By (H_4) , ones has

$$\text{Re} \left[\left(\frac{ds}{d\vartheta} \right)^{-1} \right]_{\vartheta=\vartheta_0, \mu=\mu_0} > 0. \quad (59)$$

The proof of Lemma 5.2 ends. ■

By virtue of the exploration above, the following result can be easily derived.

Theorem 5.1. *Under the hypotheses (H_3) and (H_4) , the positive equilibrium point $E(a, \frac{b}{a})$ of model (36) is locally asymptotically stable if ϑ lies in the range $[0, \vartheta^0)$ and a Hopf bifurcation will happen around $E(a, \frac{b}{a})$ if ϑ exceeds the critical value ϑ^0 .*

6 MATLAB simulation figures

In this section, we will carry out MATLAB simulation to check the correctness of Theorem 4.1 and Theorem 5.1. We give two examples.

Example 6.1. Consider the following fractional-order delayed Brusselator chemical reaction model:

$$\begin{cases} \frac{d^{0.97}v_1}{dt^{0.97}} = 0.6 - (1 + 1)v_1 + v_1^2v_2(t - \vartheta), \\ \frac{d^{0.97}v_2}{dt^{0.97}} = v_1 - v_1^2v_2(t - \vartheta), \end{cases} \quad (60)$$

Clearly, model (60) has the unique positive equilibrium point $E(0.6, 1.67)$. Making use of MATLAB software, we can determine that $\mu_0 = 3.0092$ and $\vartheta_0 = 0.82$. The conditions (H_1) and (H_2) in Theorem 4.1 are satisfied. In order to check the correctness of Theorem 4.1, we select two different delay values. Select $\vartheta = 0.75 < \vartheta_0 = 0.82$, then the MATLAB simulation figures are presented in Figures 1-4. In terms of Figures 1-4, we can distinctly see that the positive equilibrium point $E(0.6, 1.67)$ remains locally asymptotically stable situation. Figure 1 shows the variable $v_1 \rightarrow 0.6$ as the time $t \rightarrow \infty$; Figure 2 shows the variable $v_2 \rightarrow 1.67$ as the time $t \rightarrow \infty$; Figure 3 shows the relation between variables v_1 and as v_2 the time $t \rightarrow \infty$; Figure 4 shows the relation of variables v_1 and as v_2 the time t . Select $\vartheta = 0.9 > \vartheta_0 = 0.82$, then the MATLAB simulation figures are presented in Figures 5-8. In terms of Figures 5-8, we can distinctly see that model (60) will undergo a limit cycle (Hopf bifurcation) near the positive equilibrium point $E(0.6, 1.67)$. Figure 5 shows the variable v_1 will keep periodic vibration around the value 0.6 as the time $t \rightarrow \infty$; Figure 6 shows the variable v_2 will keep periodic vibration around the value 1.67 as the time $t \rightarrow \infty$; Figure 7 shows the relation between variables v_1 and as v_2 the time $t \rightarrow \infty$; Figure 8 shows the relation of variables v_1 and as v_2 the time t . Additionally, the bifurcation plots (see Figures 9-10) are given to manifest that the bifurcation point of model (60) is roughly equal to 0.82.

Example 6.2. Consider the following fractional-order controlled delayed

Brusselator chemical reaction model:

$$\begin{cases} \frac{d^{0.97} v_1}{dt^{0.97}} = 0.6 - (1 + 1)v_1 + v_1^2 v_2(t - \vartheta), \\ \frac{d^{0.97} v_2}{dt^{0.97}} = v_1 - v_1^2 v_2(t - \vartheta) + \varrho_p \left(v_2(t - \vartheta) - \frac{b}{a} \right) + \varrho_d \frac{d^s (v_2(t) - \frac{b}{a})}{dt^s}. \end{cases} \quad (61)$$

Clearly, model (61) has the unique positive equilibrium point $E(0.6, 1.67)$. Let $\varrho_p = 0.2, \varrho_d = 0.3$. Making use of MATLAB software, we can determine that $\sigma_0 = 1.8874$ and $\vartheta^0 = 0.76$. The conditions (H_3) and (H_4) in Theorem 5.1 are satisfied. In order to check the correctness of Theorem 5.1, we select two different delay values. Select $\vartheta = 0.7 < \vartheta^0 = 0.76$, then the MATLAB simulation figures are presented in Figures 11-14. In terms of Figures 11-14, we can distinctly see that the positive equilibrium point $E(0.6, 1.67)$ remains locally asymptotically stable situation. Figure 11 shows the variable $v_1 \rightarrow 0.6$ as the time $t \rightarrow \infty$; Figure 12 shows the variable $v_2 \rightarrow 1.67$ as the time $t \rightarrow \infty$; Figure 13 shows the relation between variables v_1 and as v_2 the time $t \rightarrow \infty$; Figure 14 shows the relation of variables v_1 and as v_2 the time t . Select $\vartheta = 0.85 > \vartheta^0 = 0.76$, then the MATLAB simulation figures are presented in Figures 15-18. In terms of Figures 15-18, we can distinctly see that model (61) will undergo a limit cycle (Hopf bifurcation) near the positive equilibrium point $E(0.6, 1.67)$. Figure 15 shows the variable v_1 will keep periodic vibration around the value 0.6 as the time $t \rightarrow \infty$; Figure 16 shows the variable v_2 will keep periodic vibration around the value 1.67 as the time $t \rightarrow \infty$; Figure 17 shows the relation between variables v_1 and as v_2 the time $t \rightarrow \infty$; Figure 18 shows the relation of variables v_1 and as v_2 the time t . Additionally, the bifurcation plots (see Figures 19-20) are given to manifest that the bifurcation point of model (61) is roughly equal to 0.76.

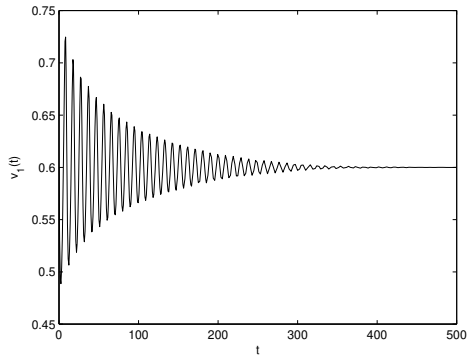


Figure 1. The MATLAB simulation result of model (60) under the delay condition $\vartheta = 0.75 < \vartheta_0 = 0.82$. The horizontal axis shows the time t and the longitudinal axis shows the variable v_1 . The variable $v_1 \rightarrow 0.6$ as $t \rightarrow \infty$.

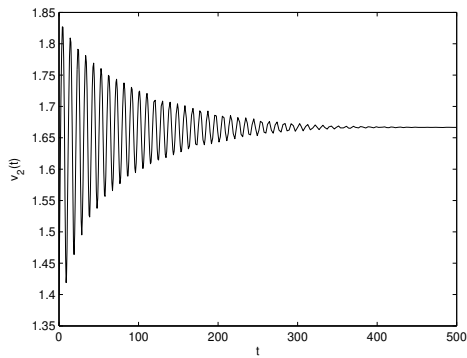


Figure 2. The MATLAB simulation result of model (60) under the delay condition $\vartheta = 0.75 < \vartheta_0 = 0.82$. The horizontal axis shows the time t and the longitudinal axis shows the variable v_2 . The variable $v_2 \rightarrow 1.67$ as $t \rightarrow \infty$.

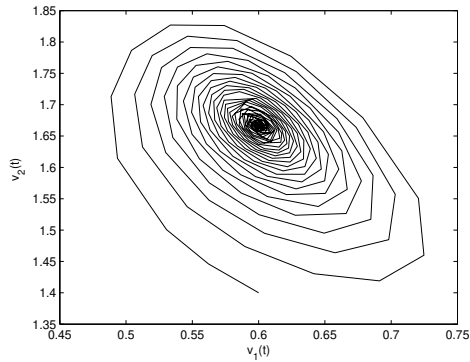


Figure 3. The MATLAB simulation result of model (60) under the delay condition $\vartheta = 0.75 < \vartheta_0 = 0.82$. The horizontal axis shows the variable v_1 and the longitudinal axis shows the variable v_2 . The variables $v_1 \rightarrow 0.6$ and $v_2 \rightarrow 1.67$ as $t \rightarrow \infty$.

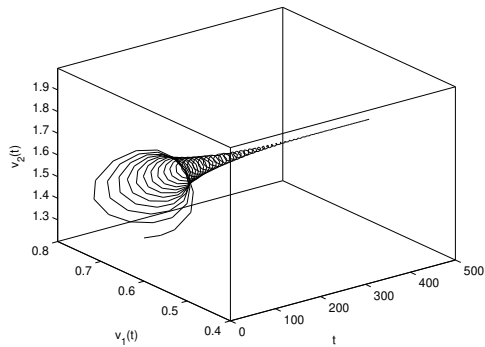


Figure 4. The MATLAB simulation result of model (60) under the delay condition $\vartheta = 0.75 < \vartheta_0 = 0.82$. The horizontal axis shows the time t , the longitudinal axis shows the variable v_1 and the vertical axis shows the variable v_2 . The variables $v_1 \rightarrow 0.6$ and $v_2 \rightarrow 1.67$ as $t \rightarrow \infty$. It shows the relation of t , v_1 and v_2 .

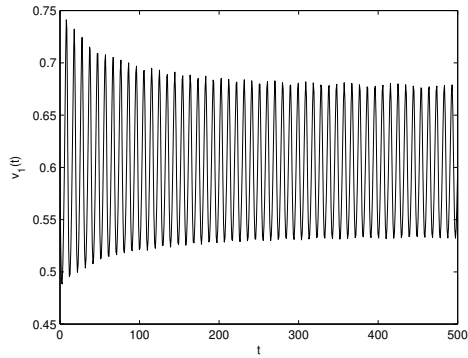


Figure 5. The MATLAB simulation result of model (60) under the delay condition $\vartheta = 0.9 > \vartheta_0 = 0.82$. The horizontal axis shows the time t and the vertical axis shows the variable v_1 . The variable v_1 will keep periodic vibration around the value 0.6 as $t \rightarrow \infty$.

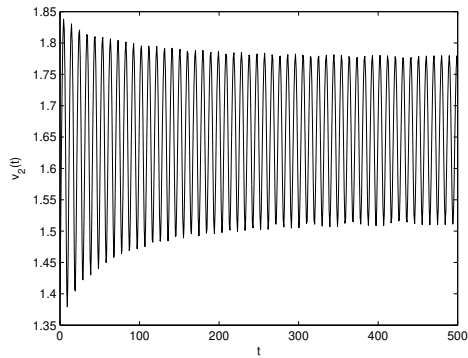


Figure 6. The MATLAB simulation result of model (60) under the delay condition $\vartheta = 0.9 > \vartheta_0 = 0.82$. The horizontal axis shows the time t and the vertical axis shows the variable v_2 . The variable v_2 will keep periodic vibration around the value 1.67 as $t \rightarrow \infty$.

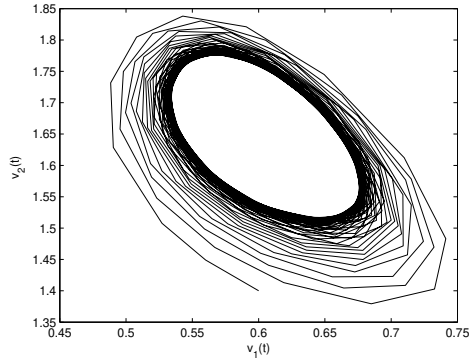


Figure 7. The MATLAB simulation result of model (60) under the delay condition $\vartheta = 0.9 > \vartheta_0 = 0.82$. The horizontal axis shows the variable v_1 and the longitudinal axis shows the variable v_2 . The variables v_1, v_2 will keep periodic vibration near $(0.6, 1.67)$ as $t \rightarrow \infty$.

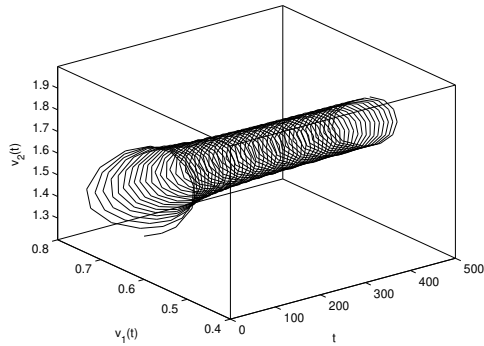


Figure 8. The MATLAB simulation result of model (60) under the delay condition $\vartheta = 0.9 > \vartheta_0 = 0.82$. The horizontal axis shows the time t , the longitudinal axis shows the variable v_1 and the vertical axis shows the variables v_1, v_2 will keep periodic vibration near $(0.6, 1.67)$ as $t \rightarrow \infty$. It shows the relation of t, v_1 and v_2 .

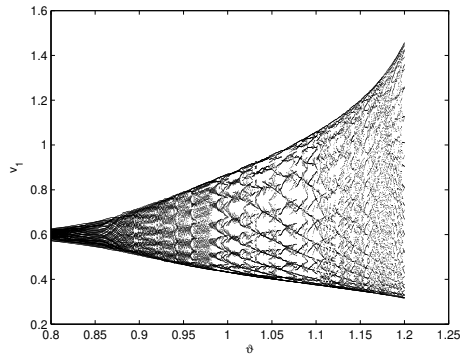


Figure 9. The bifurcation diagram of model (60). The horizontal axis shows the delay ϑ , the longitudinal axis shows the variable v_1 . The bifurcation value of model (60) is roughly equal to 0.82.

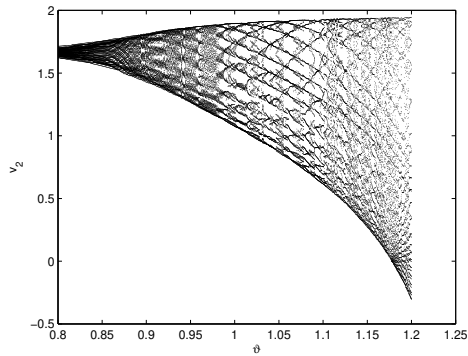


Figure 10. The bifurcation diagram of model (60). The horizontal axis shows the delay ϑ , the longitudinal axis shows the variable v_2 . The bifurcation value of model (60) is roughly equal to 0.82.

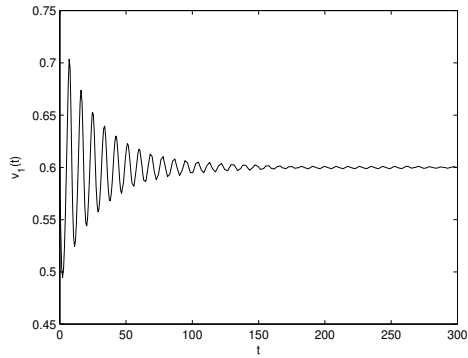


Figure 11. The MATLAB simulation result of model (61) under the delay condition $\vartheta = 0.7 < \vartheta^0 = 0.76$. The horizontal axis shows the time t and the longitudinal axis shows the variable v_1 . The variable $v_1 \rightarrow 0.6$ as $t \rightarrow \infty$.

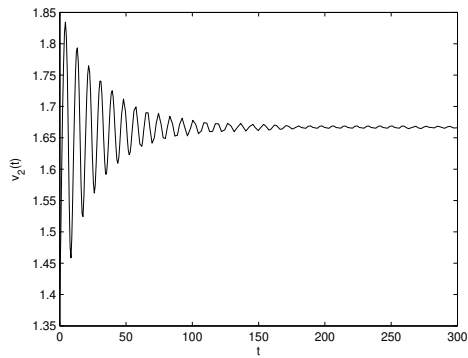


Figure 12. The MATLAB simulation result of model (61) under the delay condition $\vartheta = 0.7 < \vartheta^0 = 0.76$. The horizontal axis shows the time t and the longitudinal axis shows the variable v_2 . The variable $v_2 \rightarrow 1.67$ as $t \rightarrow \infty$.

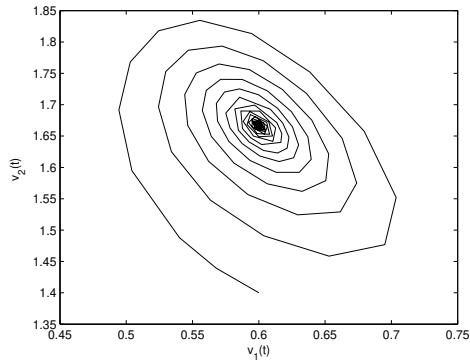


Figure 13. The MATLAB simulation result of model (61) under the delay condition $\vartheta = 0.7 < \vartheta^0 = 0.76$. The horizontal axis shows the variable v_1 and the longitudinal axis shows the variable v_2 . The variables $v_1 \rightarrow 0.6$ and $v_2 \rightarrow 1.67$ as $t \rightarrow \infty$.

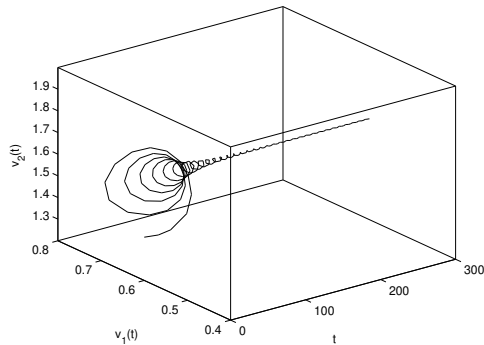


Figure 14. The MATLAB simulation result of model (61) under the delay condition $\vartheta = 0.7 < \vartheta^0 = 0.76$. The horizontal axis shows the time t , the longitudinal axis shows the variable v_1 and the vertical axis shows the variable v_2 . The variables $v_1 \rightarrow 0.6$ and $v_2 \rightarrow 1.67$ as $t \rightarrow \infty$. It shows the relation of t , v_1 and v_2 .

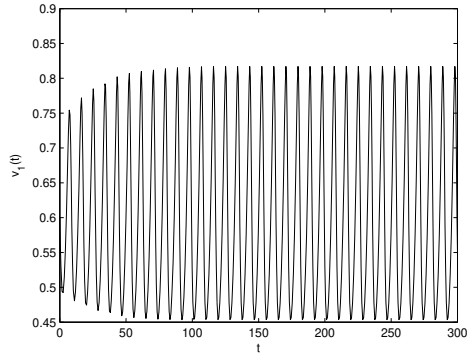


Figure 15. The MATLAB simulation result of model (61) under the delay condition $\vartheta = 0.85 > \vartheta^0 = 0.76$. The horizontal axis shows the time t and the vertical axis shows the variable v_1 . The variable v_1 will keep periodic vibration around the value 0.6 as $t \rightarrow \infty$.

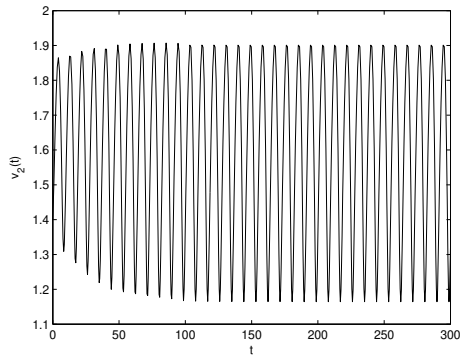


Figure 16. The MATLAB simulation result of model (61) under the delay condition $\vartheta = 0.85 > \vartheta^0 = 0.76$. The horizontal axis shows the time t and the vertical axis shows the variable v_2 . The variable v_2 will keep periodic vibration around the value 1.67 as $t \rightarrow \infty$.

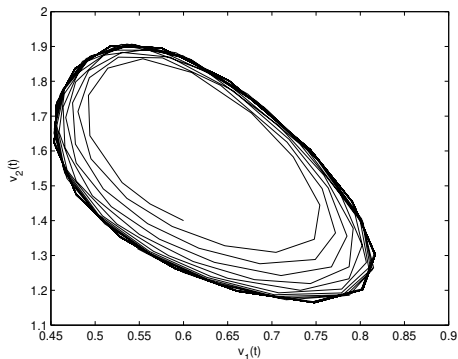


Figure 17. The MATLAB simulation result of model (61) under the delay condition $\vartheta = 0.85 > \vartheta^0 = 0.76$. The horizontal axis shows the variable v_1 and the longitudinal axis shows the variable v_2 . The variables v_1, v_2 will keep periodic vibration near $(0.6, 1.67)$ as $t \rightarrow \infty$.

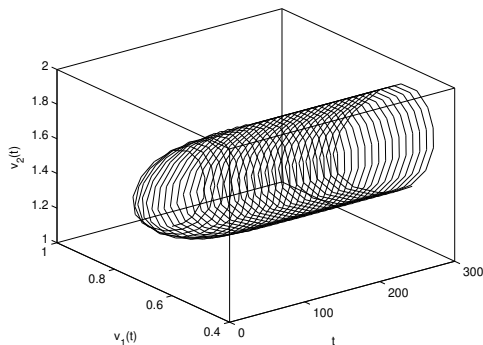


Figure 18. The MATLAB simulation result of model (61) under the delay condition $\vartheta = 0.85 > \vartheta^0 = 0.76$. The horizontal axis shows the time t , the longitudinal axis shows the variable v_1 and the vertical axis shows the variables v_1, v_2 will keep periodic vibration near $(0.6, 1.67)$ as $t \rightarrow \infty$. It shows the relation of t, v_1 and v_2 .

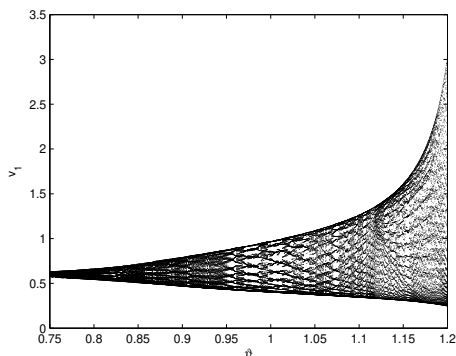


Figure 19. The bifurcation diagram of model (61). The horizontal axis shows the delay ϑ , the longitudinal axis shows the variable v_1 . The bifurcation value of model (61) is roughly equal to 0.76.

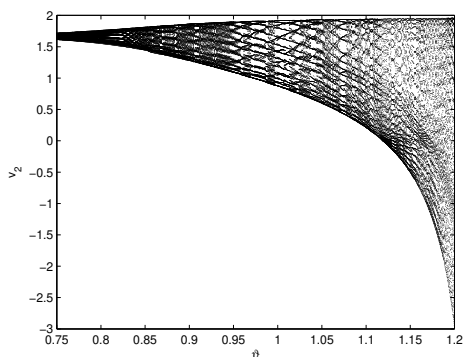


Figure 20. The bifurcation diagram of model (61). The horizontal axis shows the delay ϑ , the longitudinal axis shows the variable v_2 . The bifurcation value of model (61) is roughly equal to 0.76.

7 Conclusions

In order to inquire into the concentrations of the chemical reactants in chemistry, we set up a novel fractional-order delayed Brusselator chemical reaction model. The properties (include existence and uniqueness, non-

negativeness) of the solution of fractional-order delayed Brusselator chemical reaction model have been analyzed in detail. By virtue of Laplace transform and the characteristic equation of the fractional-order delayed Brusselator chemical reaction model, we have built a new delay-independent stability and bifurcation condition for the fractional-order delayed Brusselator chemical reaction model. The influence of delay on Hopf bifurcation of the fractional-order delayed Brusselator chemical reaction model are explored. Taking advantage of a proper PD^s controller, we can effectively control the stability and the time of occurrence of Hopf bifurcation of the fractional-order delayed Brusselator chemical reaction model. The exploration results play a vital role in dominating the concentrations of different chemical substances. The research methods have important theoretical guiding significance in many control areas.

Acknowledgment: This work is supported by National Natural Science Foundation of China (No.62062018), Project of High-level Innovative Talents of Guizhou Province ([2016]5651), Guizhou Key Laboratory of Big Data Statistical Analysis(No.[2019]5103), Basic Research Program of Guizhou Province (ZK[2022]025), Natural Science Project of the Education Department of Guizhou Province (KY[2021]031), Key Project of Hunan Education Department (17A181), University Science and Technology Top Talents Project of Guizhou Province (KY[2018]047), Foundation of Science and Technology of Guizhou Province ([2019]1051), Guizhou University of Finance and Economics(2018XZD01).

References

- [1] A. M. Zhabotinsky, Periodical process of oxidation of malonic acid solution (a study of the Belousov reaction kinetics), *Biofizika* **9** (1964) 306–311.
- [2] A. M. Zhabotinsky, Periodic liquid phase reactions, *Proc. Nat. Acad. Sci.* **157**(1964) 392–395.
- [3] R. Kapral, Discrete models for chemically reacting systems, *J. Math. Chem.* **6** (1991) 113–163.

-
- [4] C. J. Xu, W. Zhang, C. Aouiti, Z. X. Liu, P. L. Li, Bifurcation dynamics in a fractional-order oregonator model including time delay, *MATCH Commun. Math. Comput. Chem.* **87** (2022) 397–414.
- [5] C. J. Xu, C. Aouiti, Z. X. Liu, P. L. Li, L. Y. Yao, Bifurcation caused by delay in a fractional-order coupled oregonator model in chemistry, *MATCH Commun. Math. Comput. Chem.* **88** (2022) 371–396.
- [6] Q. Din, Dynamics and Hopf bifurcation of a chaotic chemical reaction model, *MATCH Commun. Math. Comput. Chem.* **88** (2022) 351–369.
- [7] X. X. Qie, Q. B. Ji, Computational analysis and bifurcation of regular and chaotic Ca^{2+} oscillations, *Math.* **9** (2021) #3324.
- [8] Q. Din, T. Donchev, D. Kolev, Stability, bifurcation analysis and chaos control in chlorine dioxide-iodine-malonic acid reaction, *MATCH Commun. Math. Comput. Chem.* **79** (2018) 577–606.
- [9] V. Voorsluijs, Y. D. Decker, Emergence of chaos in a spatially confined reactive system, *Phys. D* **335** (2016) 1–9.
- [10] L. Wang, D. Q. Jiang, G. S. K. Wolkowicz, Global asymptotic behavior of a multi-species stochastic chemostat model with discrete delays, *J. Dyn. Diff. Equat.* **32** (2020) 849–872.
- [11] I. Prigogine, R. Lefever, Symmetry breaking instabilities in dissipative systems II, *J. Chem. Phys.* **48** (1968) 1695–1700.
- [12] Q. Din, A novel chaos control strategy for discrete-time Brusselator models, *J. Math. Chem.* **56** (2018) 3045–3075.
- [13] G. Nicolis, I. Prigogine, *Self-Organizations in Non-equilibrium Systems*, Wiley, New York, 1977.
- [14] P. Gray, S. K. Scott, The brusselator model of oscillatory reactions, *Faraday Trans.* **84** (1988) 993–1012.
- [15] C. J. Xu, Z. X. Liu, L. Y. Yao, C. Aouiti, Further exploration on bifurcation of fractional-order six-neuron bi-directional associative memory neural networks with multi-delays, *Appl. Math. Comput.* **410** (2021) #126458.
- [16] C. J. Xu, W. Zhang, Z. X. Liu, P. L. Li, L. Y. Yao, Bifurcation study for fractional-order three-layer neural networks involving four time delays, *Cogn. Comput.* **14** (2022) 714–732.

-
- [17] X. J. Yang, C. D. Li, Q. K. Song, J. Y. Chen, J. J. Huang, Global Mittag-Leffler stability and synchronization analysis of fractional-order quaternion-valued neural networks with linear threshold neurons, *Neural Netw.* **105** (2018) 88–103.
- [18] B. Ghanbari, S. Djilali, Mathematical analysis of a fractional-order predator-prey model with prey social behavior and infection developed in predator population, *Chaos Solitons Fractals* **138** (2020) #109960.
- [19] C. J. Xu, Z. X. Liu, C. Aouiti, P. L. Li, L. Y. Yao, J. L. Yan, New exploration on bifurcation for fractional-order quaternion-valued neural networks involving leakage delays, *Cogn. Neurodyn.* (2022), in press, doi: <https://doi.org/10.1007/s11571-021-09763-1>.
- [20] C. J. Xu, D. Mu, Y. L. Pan, C. Aouiti, Y. C. Pang, L. Y. Yao, Probing into bifurcation for fractional-order BAM neural networks concerning multiple time delays, *J. Comput. Sci.* **62** (2022) #101701.
- [21] C. J. Xu, Z. X. Liu, M. X. Liao, L. Y. Yao, Theoretical analysis and computer simulations of a fractional order bank data model incorporating two unequal time delays, *Expert Syst. Appl.* **199** (2022) #116859.
- [22] M. Xiao, W. X. Zheng, J. X. Lin, G. P. Jiang, L. D. Zhao, J. D. Cao, Fractional-order PD control at Hopf bifurcations in delayed fractional-order small-world networks, *J. Franklin Inst.* **354** (2017) 7643–7667.
- [23] F. B. Yousef, A. Yousef, C. Maji, Effects of fear in a fractional-order predator-prey system with predator density-dependent prey mortality, *Chaos Solitons Fractals* **145** (2021) #110711.
- [24] M. Shafiya, G. Nagamani, New finite-time passivity criteria for delayed fractional-order neural networks based on Lyapunov function approach, *Chaos Solitons Fractals* **158** (2022) #112005.
- [25] S. S. Xiao, Z. S. Wang, C. L. Wang, Passivity analysis of fractional-order neural networks with interval parameter uncertainties via an interval matrix polytope approach, *Neurocomputing* **477** (2022) 96–103.
- [26] K. Udhayakumar, F.A. Rihan, R. Rakkiyappan, J. D. Cao, Fractional-order discontinuous systems with indefinite LKFs: An application to fractional-order neural networks with time delays, *Neural Netw.* **145** (2022) 319–330.

-
- [27] A. Hajipour, H. Tavakoli, Analysis and circuit simulation of a novel nonlinear fractional incommensurate order financial system, *Optik* **127** (2016) 10643–10652.
- [28] G. M. Xue, F. N. Lin, S. G. Li, H. Liu, Adaptive fuzzy finite-time backstepping control of fractional-order nonlinear systems with actuator faults via command-filtering and sliding mode technique, *Inf. Sci.* **600** (2022) 189–208.
- [29] C. J. Xu, W. Zhang, C. Aouiti, Z. X. Liu, M. X. Liao, P. L. Li, Further investigation on bifurcation and their control of fractional-order BAM neural networks involving four neurons and multiple delays, *Math. Meth. Appl. Sci.* (2021), in press, doi: <https://doi.org/10.1002/mma.7581>.
- [30] C. J. Xu, M. X. Liao, P. L. Li, S. Yuan, Impact of leakage delay on bifurcation in fractional-order complex-valued neural networks, *Chaos Solitons Fractals* **142** (2021) #110535.
- [31] C. D. Huang, J. Wang, X. P. Chen, J. D. Cao, Bifurcations in a fractional-order BAM neural network with four different delays, *Neural Netw.* **141** (2021) 344–354.
- [32] I. Podlubny, *Fractional Differential Equations*, Academic Press, New York, 1999.
- [33] C. D. Huang, J. D. Cao, M. Xiao, A. Alsaedi, T. Hayat, Bifurcations in a delayed fractional complex-valued neural network, *Appl. Math. Comput.* **292** (2017) 210–227.
- [34] Z. Odibat, N. Shawagfeh, Generalized Taylors formula, *Appl. Math. Comput.* **186** (2007) 286–293.
- [35] D. Matignon, Stability results for fractional differential equations with applications to control processing, in: *Computational Engineering in Systems and Application*, IEEE-SMC Proceed., Lille, 1996, pp. 963–968.
- [36] W. H. Deng, C. P. Li, J. H. Lü, Stability analysis of linear fractional differential system with multiple time delays, *Nonlin. Dyn.* **48** (2007) 409–416.
- [37] H. L. Li, L. Zhang, C. Hu, Y. L. Jiang, Z. D. Teng, Dynamical analysis of a fractional-order predator-prey model incorporating a prey refuge, *J. Appl. Math. Comput.* **54** (2017) 435–449.

- [38] Q. S. Sun, M. Xiao, B. B. Tao, Local bifurcation analysis of a fractional-order dynamic model of genetic regulatory networks with delays, *Neural Process. Lett.* **47** (2018) 1285–1296.